


Z. WANG  
K. SUGIOKA   
Y. HANADA  
K. MIDORIKAWA

# Optical waveguide fabrication and integration with a micro-mirror inside photosensitive glass by femtosecond laser direct writing

Laser Technology Laboratory, RIKEN – The Institute of Physical and Chemical Research, Hirosawa 2-1, Wako, Saitama 351-0198, Japan

Received: 22 January 2007 / Accepted: 4 April 2007  
Published online: 9 June 2007 • © Springer-Verlag 2007

**ABSTRACT** Photosensitive glass is a potentially important material for micro-fluidic devices that can be integrated with micro-optical components for biochemical analysis. Here, we demonstrate the fabrication of optical waveguides inside glass by femtosecond laser direct writing. The influence of the laser parameters on the waveguide properties is investigated, and it is revealed that the waveguide mode can be well controlled. The single mode is achieved at a low writing energy, while the multimode is achieved with increasing energy. In spite of a longitudinally elongated elliptical shape of the cross-sectional profile, the far-field pattern of the single-mode waveguide shows an almost symmetric profile. The measured propagation loss and the coupling loss are evaluated to be  $\sim 0.6$  dB/cm and  $\sim 1.6$  dB at a wavelength of 632.8 nm, respectively, under the conditions of 1.0–2.0  $\mu$ J pulse energy and 200–500  $\mu$ m/s scan speed. The increased optical loss is associated with a higher waveguide mode at higher writing energy. Furthermore, the integration of waveguides and a micromirror made of a hollow microplate inside the glass is demonstrated to bend the laser beam at an angle of  $90^\circ$  in a small chip. The bending loss is estimated to be smaller than 0.3 dB.

PACS 42.62.-b; 42.82.Cr; 82.50.Pt; 42.79.Gn; 42.81.Qb

## 1 Introduction

Recently, the fabrication of optical waveguides inside glass and crystal has attracted the great interest of researchers in not only material and optical fields but also biochemical fields [1–3]. Optical waveguides are one of the basic building blocks of many microphotonic devices used in integrated optics ranging from optical amplifiers, optical switches, ring resonators to interferometers, and have the potential for application in the telecommunication industry. Currently, the use of femtosecond (fs) pulsed laser writing is of great interest since this technique, unlike the continuous-wave (cw) or quasi-cw UV-exposed methods that are widely used for waveguide writing, is not limited to UV-photosensitive glass [4–8]. When intense fs pulses are tightly focused inside the volume of a transparent substrate, nonlinear absorption of

the laser energy in the focal volume takes place, leading to optical breakdown and a change in the refractive index. Although laser-induced breakdown and damage in transparent materials are well-studied subjects, the mechanism of refractive index changes is not yet completely understood [9–12]. However, a discussion on the physical mechanisms considered at present can be found, for example, in [7, 13–15]. The position where these refractive index changes occur within the substrate can be controlled in all three dimensions simply by changing the focal position using a computer-controlled *xyz*-stage. This enables the direct writing of buried optical waveguides and more complex (3D) devices with great flexibility. So far, waveguides have been written in various types of glass, including low-phonon hosts such as fluorides and highly nonlinear glass such as chalcogenides [16].

Foturan glass is a commercially available photosensitive glass that can be selectively etched with a contrast ratio of 20–50 in dilute hydrofluoric acid solution by either UV or fs laser exposure followed by heat treatment [17, 18]. We have so far succeeded in fabricating a variety of 3D hollow microstructures in this glass using the fs laser [18]. The ability to directly form 3D microstructures in this glass, along with its resistance to high temperature and corrosion, has made it a particularly attractive platform for microfluidics [18–20]. Furthermore, its high optical transparency makes it equally attractive for the fabrication of microoptical components [21]. Therefore, Foturan glass is potentially an important material for biophotonic microdevices in which microfluidics and microoptics are integrated for biosensing applications. Although fs lasers are commonly used for waveguide fabrication in many types of glass, only a limited number of studies have concentrated on waveguide writing in Foturan including proton beam writing [7, 22–24]. Furthermore, from a device perspective, this technology is still in its early stages. In particular, fabricated waveguides are yet to be completely characterized as to the optical propagation losses and the refractive index structures which are responsible for the waveguide properties, and the dependence on the fabrication parameters should also be clarified.

In this paper, we present the profiles of output light beams guided by waveguides in terms of dependence on the processing parameters of fs laser direct writing, such as scanning speed and laser energy. Propagation loss is determined for waveguides directly written in Foturan glass at a 632.8 nm

✉ Fax: +81-48-462-4682, E-mail: ksugioka@postman.riken.go.jp

wavelength of the He–Ne laser beam. Furthermore, we attempt to integrate the waveguides with a micromirror made of a hollow microplate in order to bend the laser beam in a small area, since such an optical microcomponent based on hollow structures can be easily fabricated in Foturan glass by another fs laser process [21]. The waveguide bends are crucial for minimizing the device size to enable biophotonics as well as photonics applications [25, 26].

## 2 Experimental

For the fabrication of optical waveguides in this work, the generation of refractive index changes was carried out using a commercial fs laser workstation, a 800 mW regenerative amplified Ti:sapphire laser (Clark MXR) with emission at 775 nm wavelength with a pulse duration of 150 fs and repetition rate of 1 kHz. The detailed configuration has been described elsewhere [27]. Pulse energy was adjusted using polarizer and neutral density (ND) filters. The 6 mm beam width of the output laser was reduced to 3 mm by passing it through an aperture to improve the beam quality. For the convenience of energy measurement, laser power given below used in our experiments were the values measured before the 3 mm aperture instead of on the glass substrate surface after focusing. The exact energy deposited inside the glass sample was significantly lower than this measured value. For example, the output energy of 1.25  $\mu\text{J}/\text{pulse}$  before the aperture is decreased to 0.35  $\mu\text{J}/\text{pulse}$  at the irradiation position of the sample. The focusing system was a 20 $\times$  microscope objective with a numerical aperture (N.A.) of 0.46. Optical waveguides were fabricated by moving the samples perpendicularly to the laser beam axis using a computer-controlled  $xyz$ -stage with a resolution of 0.5  $\mu\text{m}$ . The scanning speed ranged from 100  $\mu\text{m}/\text{s}$  to 5000  $\mu\text{m}/\text{s}$  at laser powers from 0.5  $\mu\text{J}/\text{pulse}$  to 5.0  $\mu\text{J}/\text{pulse}$ . The whole fabrication process was displayed on the PC monitor using a charge-coupled device (CCD). The photosensitive glass used in this study was commercially available Foturan glass from the Schott Glass Corporation, which is composed of lithium aluminosilicate doped with trace amounts of silver, cerium and antimony [28]. Commercial Foturan samples were cut and mechanochemically polished along the cut edges to achieve an optical finish. After fs laser direct writing, no annealing was performed. In order to optically characterize the waveguides, mode profile and propagation loss measurements were carried out using different laser fabrication parameters.

## 3 Results and discussion

### 3.1 Cross-sectional feature of waveguide

Figure 1 shows the optical microscope images of the cross-sectional shapes of waveguides written in Foturan glass under different writing conditions. The waveguides show a highly elliptical cross-section extending 20–80  $\mu\text{m}$  along the  $z$  direction, that is, the laser beam propagation direction, and only 4–7  $\mu\text{m}$  along the  $y$  direction; this is similar to the waveguides fabricated in Er-doped phosphate glass by fs laser direct writing [29]. Furthermore, it is observed that the structures produced in Foturan glass are influenced by the laser energy and translation scanning speed. The ellipticity is

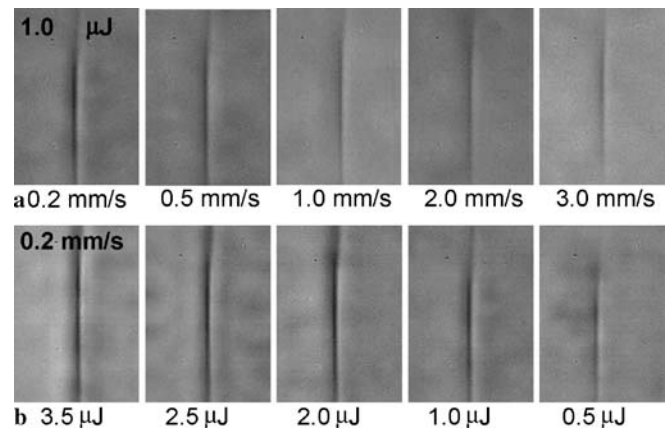


**FIGURE 1** CCD images from optical microscope observation of the cross-sectional shape of the waveguides. (a) Upper row is obtained at constant writing energy and various scan speeds. (b) Bottom row is obtained at constant scan speed with various pulse energies

reduced at lowing laser power and at higher scanning speed. However, low laser energy with high scanning speed, e.g., 0.5  $\mu\text{J}$  above 3000  $\mu\text{m}/\text{s}$  and 0.25  $\mu\text{J}$  above 1000  $\mu\text{m}/\text{s}$ , is insufficient to induce the index change in our experiments. Low speed at too lower energy, e.g., 0.125  $\mu\text{J}$ , 200  $\mu\text{m}/\text{s}$ , leads to similar results. High laser energy with low speed, e.g., 5.0  $\mu\text{J}$  below 100  $\mu\text{m}/\text{s}$ , causes damage during the modification of the refractive index in Foturan glass. For waveguide writing of inside the Foturan glass, sufficient laser energy and energy depositing time in the focal area must be tuned carefully. The suitable operating conditions under our experiments are 0.5 to 4.0  $\mu\text{J}$  laser pulse energy and 200 to 2000  $\mu\text{m}/\text{s}$  scan speed. Figure 2 summarizes the waveguide writing results in Foturan glass by fs laser irradiation under various conditions.

For the elliptical profiles of the waveguide cross-section, as discussed in previous reports [20, 23], when a fs pulse is focused inside the glass, there is a spatial correlation between the region of refractive index change and the shape of the laser energy intensity distribution around the irradiation position. The area at the irradiation position is not infinitesimally small as predicted on the basis of the geometrical optics but has a 3D intensity distribution with contours that trace out an ellipsoidal volume. This elongated depth of focusing is present in all optical systems, as is well known [30]. When

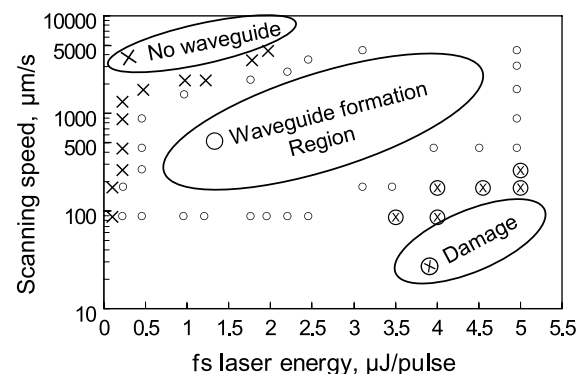


**FIGURE 2** Summary of waveguide writing results inside Foturan glass by fs laser irradiation under various conditions. Under the conditions in the regions surrounded by the circles, waveguides can be fabricated

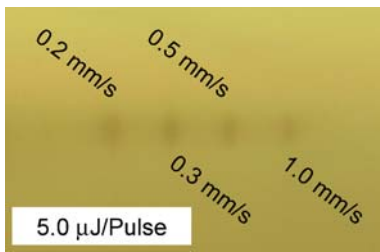


**FIGURE 3** Optical microscope image of the cross-sectional shape of the waveguides when a slit of 0.2 mm was used to adjust the energy distribution at the fs laser focal spot. The laser pulse energy was set at 5  $\mu\text{J}/\text{pulse}$

the glass material is exposed to fs laser pulses, the refractive index is locally modified within an ellipsoidal shape whose size is defined by the N.A. of the optical system and by the laser parameters such as beam waist and energy. This results in modified structures with a serious asymmetric transverse profile when the focus is translated perpendicularly to the direction of beam propagation. Because the elliptical cross-sectional shape reflects the laser energy distribution near the irradiation position, the key strategy for improving the aspect ratio is to modify the energy distribution near the laser focal spot. Although the energy distribution in the longitudinal direction at the focal spot is largely reduced when using high-N.A. oil-immersion objectives, the working distance from the glass surface is also greatly shortened to the order of several hundred micrometers. In order to reduce the aspect ratio of microchannels [20] and waveguides embedded [23] in Foturan glass, a slit is used to modify the energy distribution at the laser focus. Figure 3 shows an example in which a slit of 0.2 mm width is inserted above the objective lens; it is obvious that the elliptical cross-sectional shape is significantly improved to an almost circular shape. Different ellipticities can be achieved by adjusting the width of the slit used. It should be noted here that the laser energy of 0.5  $\mu\text{J}/\text{pulse}$  used to write the waveguide is higher than that in Fig. 1 since a large part of laser beam is shut off by the slit.

### 3.2 Guided beam profile of waveguide

To measure the guided-light profiles, a He–Ne laser beam is coupled into one of the facets of the fabricated optical waveguide using a  $\times 20$  objective lens (N.A. = 0.35). Near-field profiles are obtained by imaging the output beam at another facet of the waveguide sample. The detailed configuration of the setup used is shown in Fig. 4. By examining near- and far-field profiles, we are able to determine the optimum conditions that yield single-mode and high-output waveguides in the glass. The near-field beam profiles can be

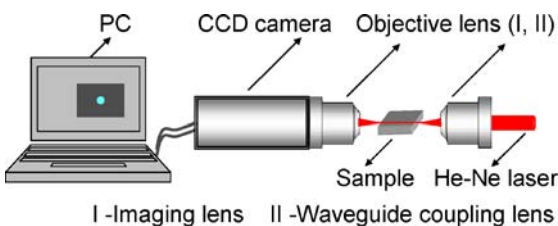


**FIGURE 4** Experimental setup used to characterize the waveguides

quite sensitive to writing parameters, as illustrated in Fig. 5. By controlling the laser writing parameters, different modes of waveguides can be produced. At low writing energy, the waveguide is the single mode; the multimode can be produced simply by either increasing the laser energy or decreasing the scanning speed. In our experiments shown here, the waveguide mode changes to the multimode above 2.5  $\mu\text{J}/\text{pulse}$  (not shown in Fig. 5), and the mode order increases with increasing pulse energy. For example, as can be seen in Fig. 5, the guided beam has two modes at 3.15  $\mu\text{J}/\text{pulse}$  and three modes at 4.55  $\mu\text{J}/\text{pulse}$  with a scanning speed of 200  $\mu\text{m}/\text{s}$ . Even though the fabricated waveguide shows an elliptical profile, both the near-field and far-field patterns of the single-mode waveguide show a symmetric profile (Fig. 5). A similar phenomenon was observed in waveguide writing using a fs laser although the details of the cause are still unclear [31].

Since, in our setup, the length of the waveguide is typically 1 cm or less, unguided light from the focused He–Ne beam interfered with the light coupled out of the waveguide, resulting in an interference pattern of concentric rings in the far field. The radius at which the fringes fade depends on the N.A. of the coupling lens and the waveguide. When the input-single pulse energy for waveguide writing is too high, visible damage of the laser modified region is easily observed. In this case, the fabricated waveguide cannot function as the optical waveguide because of the cracks or void structure, as shown in Fig. 6. These damage structures cause, for example, serious scattering and reflection within the entire waveguide.

It is well known that the optical properties of waveguides are determined by the distribution of the refractive index.

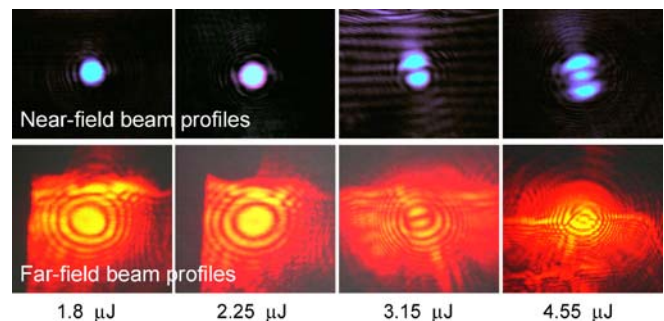


**FIGURE 5** Mode profiles of the output from the optical waveguides 10 mm long fabricated using different laser energies and 200  $\mu\text{m}/\text{s}$  scan speed

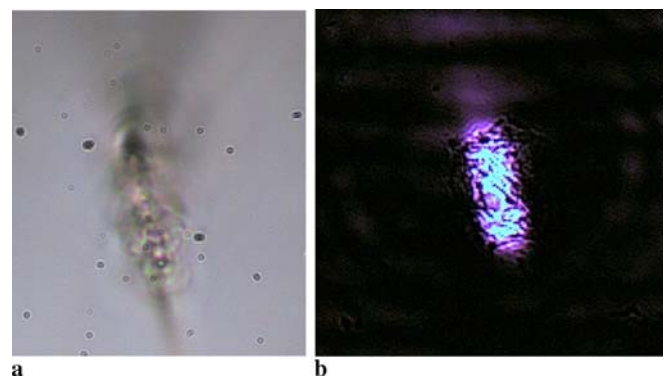


**FIGURE 6** Output profiles from the waveguides fabricated using 30  $\mu\text{J}$  pulse energy and 200  $\mu\text{m}/\text{s}$  scan speed. (a) Cross-sectional shape of the damaged waveguide. (b) Near-field beam pattern from the damaged waveguide

The maximum positive refractive index change is  $1.6 \times 10^{-3}$  for proton beam writing in Foturan photosensitive glass [22], and up to  $1.5 \times 10^{-3}$  is generated by fs laser modification at 80 fs and 1 kHz [7]. Using the measured refractive-index profiles, one can identify the modes which guide the light of a certain wavelength [4]. Inversely, the guided mode can be an indicator of the relative change of the refractive index in the laser-irradiated region. In our experiments, the waveguide cross-sectional dimensions and the amount of refractive-index change can be easily altered by adjusting either the laser energy or the writing speed, i.e., by varying the total photon dose supplied to Foturan glass (Fig. 1). At a low energy, the fs-laser-induced refractive-index change should be small, and only single-mode operation is observed. Multimode waveguides with a highly controllable mode number can be achieved at higher laser writing energy because of a higher increase of refractive-index change.

Regarding the mechanism of fs-laser-induced refractive-index changes in Foturan glass, it is known that when a two-step heat treatment is applied, Ag nanoparticles begin to aggregate in the laser-exposed region, and then a crystalline phase of Li-metasilicate is formed [18]. However, since thermal treatment is not applied in our waveguide writing, it is unlikely that the aggregation of Ag nanoparticles or the formation of a crystalline phase in the laser-irradiated area is responsible for the refractive index change. Although further studies are required to fully understand the mechanism of refractive-index change in Foturan glass, the density change in Foturan could be one possible reason [22].

### 3.3 Optical loss of waveguide

The propagation loss at 632.8 nm is evaluated by fabricating three waveguides of different lengths under the same condition in coupons separated from an identical substrate. Due care is taken to assure that identical coupling conditions are achieved for all three waveguides. Figure 7 shows the schematic illustration of the setup for evaluating the propagation loss of the fabricated waveguide. The three different samples are mounted using the same optical setup. Before measuring the power of the guided laser, the launched He–Ne laser beam is focused at the exact entrance of each waveguide with three-dimensional adjustment and rotation under observation using the CCD camera, as shown in Fig. 4, to ensure

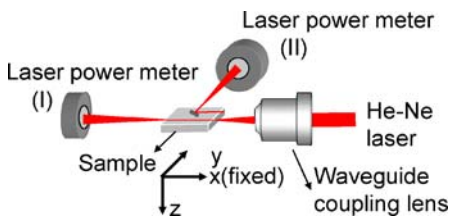


**FIGURE 7** Schematic of the setup for optical loss measurement for the guided and bent laser beam. (As in the case of Fig. 4, an imaging lens was first applied to couple the He–Ne beam into the waveguide, then the laser power meter replaced the imaging lens for output power measurement. Here, we used laser power meter I is for the straight waveguide, and laser power meter II for the bent waveguide. The bent waveguide is fabricated by integrating a waveguide with a micromirror; a detailed description is given in Sect. 3.4)

the same angular alignment for each sample. The power of the guided laser beam is measured to replace objective lens I (imaging lens) and the CCD camera in Fig. 4 by power meter I as shown in Fig. 7. The several measurements are taken for each waveguide and the average is adopted. The throughout data for optical loss as a function of waveguide length is shown in Fig. 8. Equations with linear fitting parameters are inserted for different laser writing parameters. The slope of the linear fit represents the propagation loss in dB/cm and the y-intercept gives the coupling loss from both facets of each waveguide. It is clear that the coupling loss is induced by either the unmatched size or the misalignment between the waveguide and the focused He–Ne laser beam. However, the values obtained under the different conditions shown here are quite similar and range of 1.5 to 1.6 dB. This indicates that the waveguide cross-sectional size, particularly in the transverse direction, is not markedly dispersed under the conditions used in our experiments, as seen in Fig. 1. The propagation loss is around 0.5 dB/cm under the conditions investigated. How-

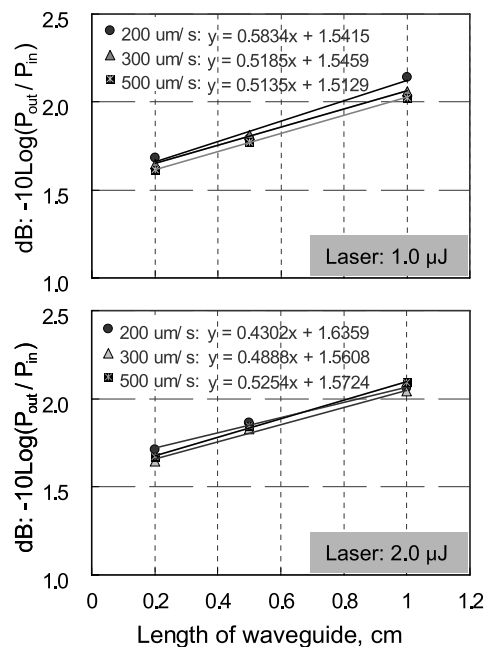


**FIGURE 8** Optical loss dependence on the length of waveguides written at different laser energies and scanning speeds. Fitted linear curves give propagation loss in dB/cm (slope) and coupling loss in dB (y-intercept); same in Figs. 9 and 11

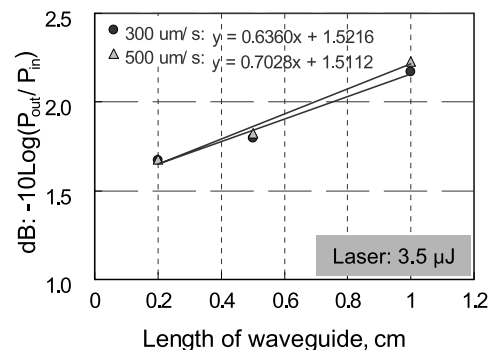


**FIGURE 9** Optical loss in dependence on the length for two-waveguides written at 3.5 μJ in pulse energy

ever, the minor difference may still indicate the possibility that the refractive index change is larger at higher energy, which would lead to a smaller propagation loss. In addition, at high energy, lowering the scanning speed leads to smaller propagation loss. Nevertheless, the throughout measurements may be within an error range that influences the accuracy. The optical loss of multimode waveguides is also measured; their coupling loss remains similar, but the large propagation loss is commensurate with the large mode profiles (Fig. 9). It is assumed that the main cause of optical propagation loss is the nonuniformity and the density fluctuation in the modified region. They may cause the different scattering, absorption, refraction and reflection in the waveguide. However, the propagation loss of around 0.5 dB/cm is still acceptable for biophotonic applications.

### 3.4 Integration with micromirror

From the practical point, a light beam guided by the waveguide is often needed to be bent when used for integration into optical and microfluidic devices. To bend the beam, a curved waveguide is commonly fabricated. In this case, the bending loss is an important issue that cannot be disregarded. To minimize the bending loss, the curvature of the curved waveguide should be larger than multiple millimeters, e.g., 5–6 mm, but this causes an undesirable increase in device size. In contrast, the integration of two straight waveguides with a mirror can significantly reduce the device size [25]. We can fabricate a micromirror made of a hollow plate inside Foturan glass by fs laser direct writing followed by thermal treatment and successive wet etching [21], and thereby can integrate the waveguides with the micromirror. Figure 10 shows the schematic illustration of the fabricated structures. We fabricated three different structures in which one waveguide (waveguide I) of a constant length is connected to the micromirror of a hollow structure with an angle of 45° and further connected to another waveguide (waveguide II) of different lengths at an angle of 90°. The experimental setup for the characterization of the integrated waveguides is the same as that for the straight waveguide shown in Fig. 7, except for use of laser power meter II instead of power meter I.

Figure 11 shows the total optical loss for the integrated waveguide with different lengths. The propagation loss is evaluated to be 0.48 dB/cm, which almost corresponds to that of straight waveguides, as shown in Fig. 8. The y-intercept gives the loss including the coupling loss and bending loss

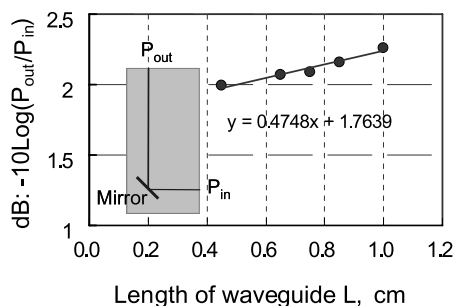


FIGURE 10 Schematic illustration of the fabricated structures used to characterize the bending loss of waveguide

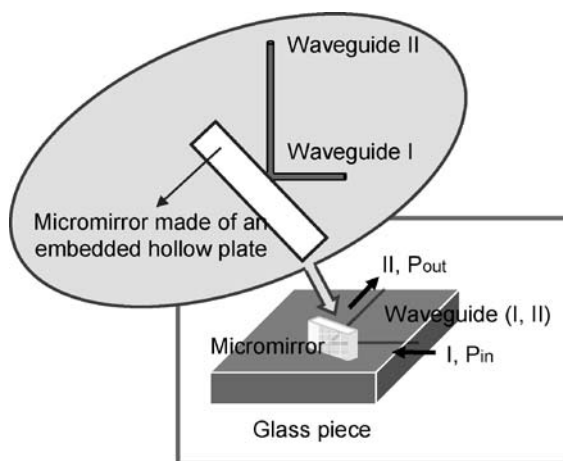


FIGURE 11 Optical loss of the waveguides integrated with mirrors, written with 1.0  $\mu$ J pulse energy and scan speed of 200  $\mu$ m/s

at the mirror. Assuming the coupling loss to be the same as that of a single straight fiber (approx. 1.5 dB), one can estimate the bending loss to be less than 0.3 dB. The bending loss may be composed of the reflection loss at the mirror and the coupling loss to the second waveguide. Two parallel mirrors integrated with three waveguides were also fabricated to form a hook-shaped structure. The evaluated bending loss increased slightly in this case because of the increase in the number of bending points.

## 4 Summary

Direct writing of waveguides in Foturan photosensitive glass has been demonstrated using a fs laser. An elliptical cross-section of waveguides was formed by the spatial laser energy distribution around the focal spot inside the glass. Waveguides with a well-controlled mode number were achieved by tuning the laser writing parameters; the single mode is produced at a low writing energy while the multimode is produced at high laser energy. The measured propagation loss and the coupling loss were evaluated to be about 0.5 dB/cm and around 1.5 dB at a wavelength of 632.8 nm, respectively, under the conditions investigated in our experiments. The optical loss increased at a higher laser energy because of a larger waveguide mode. The integration of waveguides with a mirror was realized and bending of the laser beam at an angle of 90° in a small chip with the bending loss of less than 0.3 dB was achieved. Thus, the combination of two kinds of fs laser processing, i.e., waveguide writing and 3D hollow microstructure fabrication, is very attractive for the manufacture of biophotonic microchips.

## REFERENCES

- 1 K.M. Davis, K. Miura, N. Sugimoto, K. Hirao, *Opt. Lett.* **21**, 1729 (1996)
- 2 K. Miura, J. Qiu, H. Inouye, T. Mitsuyu, K. Hirao, *Appl. Phys. Lett.* **71**, 3329 (1997)
- 3 T. Gorelik, M. Will, S. Nolte, A. Tünnermann, U. Glatzel, *Appl. Phys. A* **76**, 309 (2003)
- 4 M. Will, S. Nolte, B.N. Chichkov, A. Tünnermann, *Appl. Opt.* **41**, 4360 (2002)
- 5 C. Florea, K.A. Winick, *J. Lightwave Technol.* **21**, 246 (2003)

- 6 S. Nolte, M. Will, J. Burghoff, A. Tünnermann, J. Mod. Opt. **51**, 2533 (2004)
- 7 V.R. Bhardwaj, E. Simova, P.B. Corkum, D.M. Rayner, C. Hantovsky, R.S. Taylor, B. Schreder, M. Kluge, J. Zimmer, J. Appl. Phys. **97**, 0831021 (2005)
- 8 L. Tong, R.R. Gattass, I. Maxwell, J.B. Ashcom, E. Mazur, Opt. Commun. **259**, 626 (2006)
- 9 B. Schaffer, A. Brodeur, E. Mazur, Meas. Sci. Technol. **12**, 1784 (2001)
- 10 J.W. Chan, T.R. Huser, S.H. Risbud, D.M. Krol, Proc. SPIE **4640**, 129 (2002)
- 11 J.W. Chan, T.R. Huser, S.H. Risbud, D.M. Krol, Opt. Lett. **26**, 1726 (2001)
- 12 C.-H. Fan, J.P. Longtin, Appl. Opt. **40**, 3124 (2001)
- 13 A.M. Streltsov, N.F. Borelli, J. Opt. Soc. Am. B **19**, 2496 (2002)
- 14 C.B. Schaffer, J.F. Garcia, E. Mazur, Appl. Phys. A **76**, 351 (2003)
- 15 J.W. Chan, T.R. Huser, S.H. Risbud, J.S. Hayden, D.M. Krol, Appl. Phys. Lett. **82**, 2371 (2003)
- 16 K. Hirao, K. Miura, J. Non-Cryst. Solids **239**, 91 (1998)
- 17 T.R. Dietrich, W. Ehrfeld, M. Lacher, M. Kramer, B. Speit, Microelectron. Eng. **30**, 497 (1996)
- 18 K. Sugioka, Y. Cheng, K. Midorikawa, Appl. Phys. A **81**, 1 (2005)
- 19 A.C. Fisher, K.A. Gooch, I.E. Henley, K. Yunus, Anal. Sci. **17**, 371 (2001)
- 20 Y. Cheng, K. Sugioka, K. Midorikawa, M. Masuda, K. Toyoda, M. Kawachi, K. Shihoyama, Opt. Lett. **28**, 55 (2003)
- 21 Y. Cheng, K. Sugioka, K. Midorikawa, M. Masuda, K. Toyoda, M. Kawachi, K. Shihoyama, Opt. Lett. **28**, 1144 (2003)
- 22 A.A. Bettiol, S. Venugopal Rao, E.J. Teo, J.A. van Kan, F. Watt, Appl. Phys. Lett. **88**, 1711061 (2006)
- 23 K.J. Moh, Y.Y. Tan, X.-C. Yuan, D.K.Y. Low, Z.L. Li, Opt. Express **13**, 7288 (2005)
- 24 A.A. Bettiol, S. Venugopal Rao, T.C. Sum, J.A. van Kan, F. Watt, J. Cryst. Growth **288**, 209 (2006)
- 25 L. Li, G. Nordin, J. English, J. Jiang, Opt. Express **11**, 282 (2003)
- 26 S. Hiramatsu, T. Mikawa, O. Ibaragi, K. Miura, K. Hirao, IEEE Photon. Technol. Lett. **16**, 2075 (2004)
- 27 M. Masuda, K. Sugioka, Y. Cheng, N. Aoki, M. Kawachi, K. Shihoyama, K. Toyoda, K. Midorikawa, Proc. SPIE **4830**, 576 (2003)
- 28 H. Helvajian, P.D. Fuqua, W.W. Hansen, S. Janson, RIKEN Rev. **32**, 57 (2001)
- 29 R. Osellame, S. Taccheo, M. Marangoni, R. Ramponi, P. Laporta, D. Polli, S. De Silvestri, G. Cerullo, J. Opt. Soc. Am. B **20**, 1559 (2003)
- 30 J.J. Stamnes, *Waves in Focal Regions: Propagation, Diffraction and Focusing of Light, Sound and Water Waves* (Adam Hilger Series in Optics and Optoelectronics, Bristol, Boston, 1986)
- 31 T. Nagata, M. Kamata, M. Obara, Appl. Phys. Lett. **86**, 2511031 (2005)